Accepted Manuscript

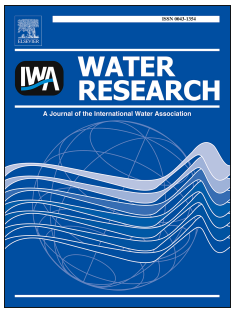

Electrochemical inactivation of bacteria with a titanium sub-oxide reactive membrane

Shangtao Liang, Hui Lin, Mussie Habteselassie, Qingguo Huang

PII: S0043-1354(18)30631-6

DOI: 10.1016/j.watres.2018.08.010

Reference: WR 13986

To appear in: *Water Research*

Received Date: 20 April 2018

Revised Date: 3 August 2018

Accepted Date: 4 August 2018

Please cite this article as: Liang, S., Lin, H., Habteselassie, M., Huang, Q., Electrochemical inactivation of bacteria with a titanium sub-oxide reactive membrane, *Water Research* (2018), doi: 10.1016/j.watres.2018.08.010.

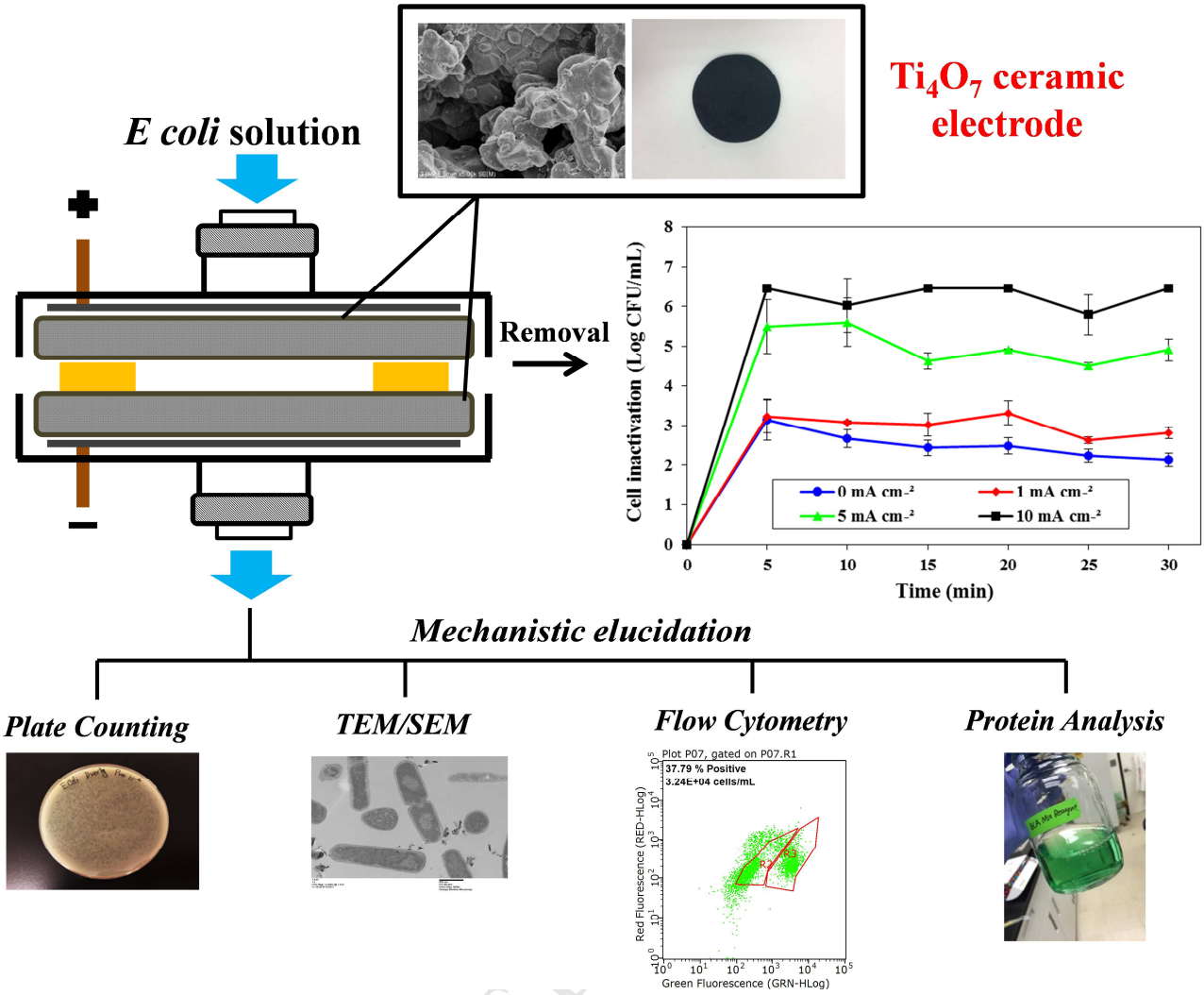

Electrochemical Inactivation of Bacteria with a Titanium Sub-oxide Reactive Membrane

Shangtao Liang[a,c], *Hui Lin*[b*], *Mussie Habteselassie*[a], *Qingguo Huang*[a*]

[a] College of Agricultural and Environmental Sciences, Department of Crop and Soil Sciences, University of Georgia, Griffin, GA 30223, United States

[b] Research Center for Eco-Environmental Engineering, Dongguan University of Technology, Dongguan 523808, P.R. China

[c] AECOM Environment, Atlanta, GA 30309

[*] Corresponding authors. Qingguo Huang, qhuang@uga.edu; Hui Lin, linhui@dgut.edu.cn

Abstract

A reactive electrochemical membrane (REM) system was developed with titanium suboxide microfiltration membrane serving as the filter and the anode, and was examined to inactivate *Escherichia coli* (*E. coli*) in water at various current densities. After passing through the membrane filter, the concentration of *E. coli* decreased from 6.46 log CFU/mL to 0.18 log CFU/mL. The REM operation and effects, including membrane pressure, anode potential, protein leakage, and cell morphology, were characterized under different treatment conditions. It was found that several mechanisms, including membrane sieving, external electrical field influence, and direct oxidation, functioned in concert to lead to bacteria removal and inactivation, and direction oxidation likely played the major role. As revealed by scanning electron microscope and extracellular protein analysis, high current density and voltage caused severe cell damage that resulted in partial or complete cell disintegration. The removal of a model virus, bacteriophage MS2, was also investigated at the current density of 10 mA cm^{-2} and achieved 6.74 log reduction compared to the original concentration (10^{11} PFU/mL). In addition to illustration of mechanisms, this study may provide a potentially promising approach that is suitable for decentralized treatment to meet dispersed water disinfection needs.

Keywords:

Reactive Electrochemical Membrane; Microfiltration; Pathogens; Water Disinfection

Introduction

According to a World Health Organization report (W.H.O., 2015), 663 million people still lack access to safe water in 2015, and most of them live in developing countries and rural areas. Waterborne pathogens can cause severe disease and death, thus remaining a primary threat to public health. Due to various limitations, the conventional disinfection methods, such as chlorination, ozonation, and UV irradiation, are implemented in centralized water treatment plants, but cannot meet dispersed disinfection needs. Additionally, ozonation and chlorination have the disadvantage of producing carcinogenic disinfection by-products (DBPs) (Li et al. 2016, Rajab et al. 2015, Schaefer et al. 2015). Therefore, there is a critical demand to develop disinfection technologies for decentralized treatments that are effective in removing waterborne pathogens, in addition to being inexpensive and easy to use.

Membrane filtration is the most commonly used water disinfection technology for decentralized uses at present, but it merely physically separates pathogens from water without killing them, and thus any operation failure could cause serious health risks. The development of biofilm on the membrane causes blockage, resulting in the need of regular filter replacement to ensure disinfection efficiency (Brady-Estévez et al. 2010, Gkotsis et al. 2014). This adds up to the maintenance cost, and thus makes membrane filtration less favorable in the long run. A technology that can simultaneously remove and inactivate pathogens is needed, and when coupled with membrane technology, it can reduce biological fouling and extend the service life of membrane filter.

Electrochemical inactivation of microbes has been long explored for decentralized water disinfection. It is particularly promising for dispersed disinfection uses at rural places because electrochemical inactivation can be operated in compacted mobile units, has high disinfection

efficiency, requires low energy consumption, and can be potentially powered by solar energy. Different electrode materials have been studied for electrochemical inactivation (Bruguera-Casamada et al. 2016, Drees et al. 2003, Jeong et al. 2009, Li et al. 2016, Rajab et al. 2015, Wen et al. 2017). However, in most of those studies, disinfection relied on electrochemically generated chlorinated oxidative species, thus toxic disinfection by-products were inevitably formed (Schaefer et al. 2015).

Reactive electrochemical membrane (REM) system has been developed in recent years, which improved disinfection efficiency and addressed the issue of DBP formation. A conductive porous material is used both as a membrane and an anode in a REM system. Traditionally, REM has been studied for applications to reduce biofouling based on cathodic potential (Elangovan and Dharmalingam. 2016). Recently, a REM system using multi-walled carbon nanotubes (MWNT) as the filter has exhibited complete inactivation of both bacteria and virus by applying 2 to 3 V cell voltage (Rahaman et al. 2012, Vecitis et al. 2011). However, this particular REM application may be limited by the disputable toxicity of carbon nanotubes and the limited service life of the filters prepared in a non-reusable manner. A commercially available porous titanium suboxide material has also be studied in REM setup using *E. coli* as a model pathogen in chloride-free solutions (Guo et al. 2016). The disinfection effects were attributed to electrostatic adsorption of bacteria on the electrode surface and the strong acidic or alkaline conditions in the near-electrode microenvironment, while direct or indirect oxidation was not considered as a major cause. The sub-stoichiometric titanium oxide material is suitable for REM applications also because of its non-toxic nature and its physical, chemical, and electrochemical stabilities. It is however imperative to better understand the mechanism of disinfection and the controlling factors for design and optimization of REM process based on titanium suboxide material.

The mechanisms that have been proposed to explain the electrochemical inactivation of bacteria include (1) indirect oxidation; (2) direct oxidation; (3) permeabilization by transmembrane potential; and (4) electroporation (Drees et al. 2003, Jeong et al. 2009, Long et al. 2015, Rajab et al. 2015). Indirect oxidation has been proposed as the primary cause of bacteria inactivation in several studies. It occurs via the electrochemically generated reactive oxidizing species (Cl_2, HClO, ClO^-, OH•, H_2O_2, and O_3), while, in chloride-free solutions, OH• is the major species responsible for bacteria inactivation (Jeong et al. 2009). A recent study indicates that reactive oxidants and electric field act synergistically in inactivating microorganisms (Bruguera-Casamada et al. 2016). Direct oxidation happens when membrane proteins and functional groups lose electrons on anode, causing lipid peroxidation and thus compromising cell integrity (Long et al. 2015). Additionally, it was reported that transmembrane potential is induced when cells are exposed to external electric field (de Lannoy et al. 2013, Huo et al. 2016). In a pulsed electric field study, transmembrane potential above 1 V and longer pulse time led to irreversible membrane damage and cell death (Pillet et al. 2016). Electroporation is a process usually associated with nanomaterials as electrodes, where a strong electric field (1-10 kV/cm) is formed at the tip of a wire- or rod-shaped nano particle, causing lethal damage to cells in touch (Huo et al. 2016, Liu et al. 2013, Liu et al. 2014, Wen et al. 2017).

An electrochemical disinfection process, depending on electrode type and treatment conditions, often involves two or more mechanisms acting simultaneously to inactivate pathogens. However, because limited electrode materials can produce large amount of OH• while sustain high voltages, most previous studies have focused on indirect oxidation in chloride-containing solution, although formation of DBPs is considered problematic (Cui et al. 2013, Huang et al. 2016, Jeong et al. 2009, Rajab et al. 2015). The recent finding of Magnéli phase

Ti_4O_7 ceramic material enabling REM with pathogen inactivation in chloride-free solutions (Guo et al. 2016) shows great promise for decentralized water disinfection, but a comprehensive study is needed to further elucidate the pathogen inactivation mechanisms involved in the process, and explore key factors governing the disinfection effectiveness.

The electrochemical inactivation of *E. coli* in Na_2SO_4 solution was investigated using a REM system with Magnéli phase Ti_4O_7 ceramic membrane operated in dead-end filtration mode under different conditions to assess the disinfection effectiveness and governing factors. The electrode material was thoroughly characterized in respect to elemental composition, crystal morphology, porosity, permeability, oxygen evolution potential, and reusability. Additionally, the pathogen inactivation mechanisms of this novel electrode material were explored by examining the change of *E. coli* over the electrochemical treatment in cell integrity and viability, surface and morphology.

Materials and methods

1. Electrode fabrication and characterization

Magnéli phase Ti_4O_7 ceramic material was produced from Ti_4O_7 nano powder, which was generated by reducing TiO_2 powder at high temperature (950 ^oC) under hydrogen flow. Subsequently, the Ti_4O_7 nano powder was mixed with binder (polyacrylamide/polyvinyl alcohol, 95/5, m/m) and 5% of water to form a slurry, which was spray-dried to small granulates before being pressed into a mold to form a compacted green body. The green body was sintered under vacuum with temperature increasing from 85 ^oC to 1250 ^oC, to first release the binder and then develop a 3 mm (thickness) × 3 cm (diameter) porous ceramic disc with a porosity of 23% and a median pore diameter of 7.5 µm (based on volume) or 4.5 µm (based on area), and an average

pore diameter of 5.7 µm. The physical and electrochemical properties of this electrode material made in house were characterized, and the results and methods used were described in Supporting Information.

2. Chemicals and strains

All chemicals used in this study were reagent-grade and obtained from Sigma-Aldrich (St. Louis, MO). All solutions were prepared with deionized water generated from Thermo Scientific Barnstead NANOpure water purification system (Waltham, MA) with a resistivity of 18 MΩ cm. *E. coli* (ATCC 15597) and *E. coli* bacteriophage MS2 (ATCC 15597-B1) were obtained from American Type Culture Collection (ATCC) (Manassas, VA).

3. Inactivation of *E. coli* with REM in dead-end filtration mode

E. coli was used as the test organism for this study. An REM device (**Figure 1**) constructed in house was operated in dead-end filtration mode with solutions inoculated with *E. coli* to evaluate the electrochemical pathogen inactivation. The REM device consists of two Ti_4O_7 ceramic membrane disk (3 cm in diameter) as the anode and the cathode, respectively, separated by a rubber ring to form an inter-electrode gap of 5 mm. All electrochemical experiments were conducted in 0.05 M Na_2SO_4 as supporting electrolyte, which is stable within the voltage range applied in this study. The electrolytic cell was powered by a controllable DC power source (Electro Industries Inc., Monticello, MN). Electrochemical filtrations were conducted by passing 150 mL of *E coli* suspension (~10^6 CFU/mL) at the flow rate of 5 mL/min using a peristaltic pump through the REM device with the membranes supplied by direct electric current at different current density (0, 1, 5, or 10 mA cm^{-2}). The effluent samples were collected every five minutes and immediately cultured on Luria-bertani (LB) agar plates to determine cell concentrations. To investigate the viability of cells on the membrane, both anode and cathode

were extracted after each filtration process using 10 mL of 0.9% sterilized NaCl solution under continuous shaking at 120 rpm for one hour to detach the cells from the membrane. The *E. coli* concentration in the effluent, membrane extract, and controls were measured using standard plate count method. Briefly, serial dilutions of samples were prepared with 0.9% saline solution prior to plating. Then, 100 µL aliquot of sample was spread plated over a LB agar plate and incubated at 37 ^{o}C for 24 h. After incubation, the number of colonies formed on the agar plate was counted and expressed as colony forming unit per mL (CFU/mL). Every sample was quantified in triplicate plates, and the average cell counts were plotted.

4. Electrochemical *E. coli* inactivation in batch reactor

Batch reactor experiments were conducted for comparison, and they were performed in a one-compartment electrolytic cell (10 cm × 5 cm × 5 cm) with the same electrodes (two Ti_4O_7 ceramic membrane disks) and the same inter-electrode gap (5 mm) as in the filtration system. In each treatment, 150 mL of *E. coli* suspension (~10^6 CFU/mL) in 0.05 M Na_2SO_4 background electrolyte was placed in the electrolytic cell with continuous stirring. A direct current was supplied at different current density (0, 1.0, 5.0 or 10.0 mA cm^{-2}) with a controllable DC power source (Electro Industries Inc., Monticello, MN). Triplicate samples were withdrawn from each reactor at time zero and after 30 minutes, and 100 µL of each sample was cultured on plate for cell density quantification during 2 h of electrolysis.

5. Cell characterization

The following cell characterizations were performed on selected treatment samples and corresponding control samples in order to explore possible pathogen inactivation mechanisms.

Protein leakage. Possible leakage of intracellular protein from *E. coli* cells was measured using Pierce™ bicinchoninic acid (BCA) protein assay kit (Thermo Scientific, Waltham, MA) as described by the manufacturer. Briefly, the test was conducted by mixing 0.1 mL of sample with 2 mL BCA working reagent and then incubating at 37 ^{o}C for 30 minutes. The 562 nm absorbance developed in each tube was measured using a Beckman Coulter DU 800 spectrophotometer (Brea, CA). A standard curve prepared with albumin standard solution was used to determine the protein concentration of each sample.

Flow cytometry. Flow cytometry analysis was performed on selected effluent samples using the Guava easyCyte™ single sample flow cytometer (EMD Millipore, Hayward, CA, USA). The LIVE/DEAD™ BacLight™ Bacterial viability kit (L34856, Invitrogen, Eugene OR, USA) containing the SYTO 9 and propidium iodide dyes were used for staining live and dead bacterial cells in both treatment and control samples. The untreated *E. coli* suspension (10^6 CFU/mL) served as the control for detection of live cells, and heat-killed cells were used as the control for detection of dead cells.

Cell morphology. *E. coli* cells in effluent samples and on membrane electrodes were fixed in 2% glutaraldehyde to preserve the cell morphology. Transmission electron microscope (TEM) observations were made using a JEOL JEM 1011 (JEOL, Inc., Peabody, MA, USA) system at 80 kV. The morphologies of the cells on membrane were also investigated using a FEI Teneo (FEI Co., Hillsboro, OR), a Field Emission Scanning Electron Microscope (FESEM), with an accelerating voltage at 5 kV.

6. Electrochemical inactivation of bacteriophage MS2

The electrochemical inactivation of bacteriophage MS2 was conducted using the same dead-end filtration device at 10 mA cm^{-2} current density. In total, 150 mL MS2 suspension (~10^{11} Plaque Forming Unit (PFU)/mL) was passed through the filter at the flow rate of 5 mL/min, and the effluent was collected for virus quantification.

After electrochemical treatment, the influent and effluent samples were quantified for MS2 titer using a plaque forming assay. Basically, the samples were subjected to ten-fold serial dilution in tryptone broth, and 0.1 mL of each of the ten diluted samples (from 1-fold to 10-fold) was mixed with 0.9 mL tryptone soft agar containing *E. coli* (ATCC 15597) host cells at 45 ^{o}C. Then the tubes were mixed and poured into the petri dishes, which would create a thin layer of agar that had been inoculated with host bacteria and MS2 in each plate. All plates were incubated for 24 hours at 37 ^{o}C. After incubation, patches of dead bacteria would form small clear spots called plaques on the plates, and each plaque represents one virus. By carefully counting the exact number (ideally between 30 and 300) of plaques on the plates, the MS2 concentrations were calculated and expressed as plaque forming units per mL (PFU/mL).

Results and Discussion

1. Characterization of Magnéli phase Ti_4O_7 membrane

The chemical composition of electrode material was assessed based on X-ray diffraction pattern (XRD) spectra (**Figure S1 and Figure S2-A**). The predominant phase of titanium suboxides in this electrode was Ti_4O_7 (~77%) and Ti_5O_9 (~23%). It is known that Ti_4O_7 exhibits the highest conductivity among all titanium suboxide phases, comparable to graphite (Smith et al. 1998), and thus the high content of Ti_4O_7 ensures favorable electrochemical performance. The electrical conductivity of our materials was measured to be 38.5 S cm^{-1} (using four point probe

212 method), which is about three orders of magnitude higher than Boron Doped Diamond (BDD)
213 electrodes (Ficek et al. 2016). The surface morphology of Ti_4O_7 ceramic membrane was shown
214 in SEM image (**Figure S2-B**), suggesting interconnected pores of various diameters. The porous
215 property (23% porosity) of the electrode provides large surface area for ROS generation, and
216 allows for size exclusion of contaminants and cells with different sizes. The tortuosity of this
217 material was estimated to be 1.98 based on an empirical correlation between tortuosity and porosity
218 developed for inert porous materials (Boudreau. 1996). Since tortuosity extends the length of path that
219 cells need to pass through and increases the chance of cell capture, depth filtration has been identified as
220 an important mechanism for regular porous beds to entrap and retain bacteria from fluids (Marty et al.
221 2014; Olson et al. 2005). The results of mercury intrusion porosimetry also indicated that the pores
222 of a wide range of diameters co-exist in the Ti_4O_7 membrane (**Figure S2-C**). Macropores appear
223 to dominate, favoring the permeability and mass transfer efficiency of the membrane. It was
224 reported that macropores are beneficial in promoting the transfer of chemicals towards the
225 electrode surface for reaction (Kong et al. 2002). The specific surface area of the porous Ti_4O_7
226 material was measured to be 0.06 m^2 g^{-1} (**Figure S2-E**), roughly 1300 times of the nominal
227 geometric area. Also, high percentage of macropores in Ti_4O_7 membrane contributes to high
228 water flux rate (12895 LMH Bar^{-1}) (**Figure S2-D)**, about five times higher than the general ultra-
229 filtration membranes used for drinking water filtration (Leiknes et al. 2004). Water permeability
230 of a membrane material is directly related to its applicability in water treatment applications, and
231 therefore the macroporous nature of the Ti_4O_7 membrane makes it promising for point-of-use
232 water treatment in filtration mode.

233 Electrochemical stability is one factor determining the service life of an electrode. For
234 example, metal oxide electrodes are usually subjected to different levels of passivation caused by
235 accumulation or precipitation of non-conductive chemical species on electrode surface

(Rajeshwar et al. 1994). In this study, the redox stability of Ti_4O_7 was demonstrated using continuous cyclic voltammetry scanning, and the electrochemical performance remained unchanged after 200 cycles of scanning (**Figure S3-B**).

2. Electrochemical inactivation of *E. coli*

An REM system (**Figure 1**) equipped with two Ti_4O_7 membrane electrodes was operated in dead-end filtration mode to investigate the electrochemical inactivation of *E. coli* under various current densities. Before regular tests, a preliminary study was conducted to assess the viability of *E. coli* in both 0.05 M Na_2SO_4 and 0.15 M (0.9% w/w) NaCl solutions, which offer ionic strengths similar to natural fresh water (McCleskey et al. 2011), and the cell concentration was found to be stable within 3.5 hours of incubation (**Figure S4**). Therefore, saline water (0.9% w/w NaCl) was utilized as the diluent in plate counting procedure to maintain cell integrity and viability. To avoid the effects of reactive chlorine species, 0.05 M Na_2SO_4 was used as background electrolyte for all experiments. Sodium sulfate (Na_2SO_4) is present in aquatic systems and inert during electrochemical processes under our test conditions.

The cell concentration in the effluent was monitored for 30 min of REM treatment at current densities ranging from 0–10 mA cm^{-2} (**Figure 2**). As shown, the concentrations of *E. coli* were reduced by more than 2, 3, 4, and 6 log units at the current densities of 0, 1, 5, and 10 mA cm^{-2}, respectively, at the first sampling point of 5 minutes, and the inactivation effect lasted through the 30-min monitoring period. When no electric power was applied to the device (0 mA cm^{-2}), *E. coli* cells were removed solely by physical separation through depth filtration. The predominant pores in Ti_4O_7 ceramic membrane have diameters between 3 to 10 μm (**Figure S2-C**), thus some of them are capable of capturing *E. coli* cells with a typical size of 0.5 μm in width and 2 μm in length. In addition, the tortuosity of the materials resulting from interconnected

pores of various sizes can significantly extend the distance that cells travel and increase the chance of being captured. Similarly, 1 log reduction in *E. coli* concentration was observed in the permeate solution from a cross-flow filtration system with a tubular Ti_4O_7 electrode, presumably through bacteria adsorption and size exclusion (Guo et al. 2016). Although the average pore size of the tubular electrode material in the earlier study was 1.7 μm, smaller than the average pore size (5.7 μm) of the Ti_4O_7 membrane electrodes in this study, the depth filtration effect was not as good as the 2.25 log reduction observed in this study. This might be due to that a much higher transmembrane pressure used during the cross-flow filtration, which might force more cells to pass through membrane. Moreover, the interconnected pores of various diameters (**Figure S2-C**) may lead to a greater tortuosity of the membranes in this study, which in combination with the slightly larger thickness (3 mm vs. 2.5 mm) may have caused the enhanced filtration efficiency. Increasing current density from 0 to 1 mA cm^{-2} enhanced the inactivation of bacteria by less than 1 log unit, which was most likely contributed by the electrostatic adsorption between the negatively charged bacteria and the anode surface with an opposite charge.

The pathogen inactivation effect was significantly enhanced from 4.88 log to 6.28 log when the current density was raised to 5 mA cm^{-2} and 10 mA cm^{-2}, respectively, which is consistent with previous studies of different electrode types (Guo et al. 2016, Pillet et al. 2016, Rahaman et al. 2012, Raut et al. 2014, Schmalz et al. 2009, Vecitis et al. 2011). Higher current density is associated with higher anodic potential as shown in the linear voltammetry scanning (**Figure S3-A**), and the oxygen evolution potential (OEP) is at 1.3 V (*vs. NHE*), at and beyond which oxygen is produced on anode with stronger ROS production as well (Enache et al. 2009, Marselli et al. 2003). As shown in **Table 1**, the cell voltages applied to the REM system for disinfection experiments were 6.4 V, 7.6 V and 9.5 V at current density of 1 mA cm^{-2}, 5 mA cm^{-2}

and 10 mA cm^{-2} respectively. According to a correlation between anodic potential and cell potential measured in a three-electrode system (**Figure S5)**, these cell voltages corresponded to the anodic potentials of 2.15 V, 2.52 V, and 3.43 V, respectively, among which the latter two (5 mA cm^{-2} and 10 mA cm^{-2}) were above the OEP (1.3 V *vs. NHE*), and thus would effectively generate hydroxyl radicals and other ROS, but not at 1 mA cm^{-2}. The effective production of hydroxyl radicals at Ti_4O_7 anode above oxygen evolution potential has been documented and confirmed in our recent study using salicylic acid as the radical scavenger (Liang et al. 2018). Although hydroxyl radical is the most powerful disinfectant that can be electrochemically generated, weaker ROS, such as H_2O_2 and O_3, may also be formed (Cui et al. 2013, Sultana et al. 2015). All such ROS species are effective for pathogen inactivation because of their ability to alter cell membrane permeability and cause cell rupture.

No significant variation in pH (~6.5) was observed in effluent samples collected during the REM treatment at various conditions (data not shown). This indicated that, in this undivided electrolytic reactor setup, the protons formed on the anode from water hydrolysis was counterbalanced by the hydroxyl ion produced on cathode, or the oxidants generated at anode were reduced back to water at cathode. Thus, the change in acidity or alkalinity that was proposed to be the factor causing bacteria inactivation in the earlier study with a divided electrolytic cell setup (Guo et al. 2016) was not the case in this study. It is worth noting that a few previous studies have indicated that *E. coli* cells did not undergo any kind of inactivation within 60 minutes at acidified conditions (pH ~ 3) (Bruguera-Casamada et al. 2016, Geveke and Kozempel 2003). Indeed, certain species of *E. coli* can tolerate a rather wide range (3.7 ~ 8.0) of pH (Presser et al. 1997).

The pressure of the peristatic pump for solution delivery during the course of REM treatment was monitored, and the result was shown in **Figure S6**. As indicated, the initial pressures for the treatments at 5 mA cm^{-2} and 10 mA cm^{-2} are higher than those at 0 mA cm^{-2} and 1 mA cm^{-2}, and reached plateau much faster. This is probably due to the gas generation on the electrodes at high current densities as mentioned above. As evidenced by TEM images (discussed below), cell debris was generated during the high current treatments (5 and 10 mA cm^{-2}) that caused severe damage to cells. Cell debris may also accumulate in the tortuous channels in the membrane, forming clogs and thus causing pressure drop to ramp up over time. The trend of the increasing pressure at 0 mA cm^{-2} over time indicates the accumulation of bacteria mass on the membranes. It is therefore critical to investigate the quantity and viability of cells on membrane to evaluate the efficiency of the REM system to inactivate *E. coli*. The membrane electrodes (both anode and cathode) were extracted in 10 mL 0.9% NaCl for one hour to remove the bacteria after each operation and the concentration of *E coli* in extract were determined (**Figure S7**). In general, the concentration of the viable cells in the extracts was lower as the applied current density increased, although those from 1 and 5 mA cm^{-2} treatments were close. In **Table 1**, we listed the total number of live cells detected on membrane as well as in effluent, and they were expressed as percentage comparing to the number of cells delivered to the filtration device within the total 30 minutes of test. The total bacteria removal were thus calculated as 99.640%, 99.895%, 99.981%, and 99.998% for 0, 1, 5, and 10 mA cm^{-2} treatments, respectively. The mechanisms that may have caused such significant levels of disinfection have been explored and elucidated below. It should be noted that the energy consumption values listed in **Table 1** were calculated based on our bench scale tests. The energy-efficiency could be further

optimized for applications by using larger scale reactor operated at high flow rates and equipped with better electric circuit that involves less ohmic loss.

For comparison, the electrochemical inactivation of *E. coli* was also evaluated in a batch reactor setup using the same Ti_4O_7 ceramic electrodes used in the REM study. No apparent reduction in cell density was found in the batch reactor at zero current density (**Figure 3**), unlike the REM treatment, where the cell concentration was reduced by more than 2 log. This result suggested that physical adsorption of *E. coli* cells on the electrode was negligible, and that they were held on the membrane electrodes primarily by depth filtration in REM treatment. No significant bacteria inactivation was found at 1 mA cm^{-2} in the batch reactor either. Increasing current density to 5 and 10 mA cm^{-2} resulted in significant inactivation of *E. coli* at 1.37 and 2.05 log reduction, respectively, but much lower than the log reduction (4.88 log and 6.28 log) achieved in REM treatment at the same current density. The greater disinfection effect in the REM process in comparison to the batch reactor operation may results from the convection-facilitated mass transfer during filtration in REM (Vecitis et al. 2011, Zaky and Chaplin 2014), where the cells were forced to pass through the interconnected pores in the electrodes, thus increasing their chance to get in contact with ROS generated also on the electrode surface. The significant bacteria inactivation during REM, in particular at 10 mA cm^{-2} current density, is discussed in more detail below.

3. Possible disinfection mechanisms during REM treatment

In selected REM treatments, the protein concentration in the effluent was monitored as an indicator of membrane permeability alteration to assess protein leakage. As shown in **Figure 4** the protein level remained stable at zero-current control. Increasing current density to 1 mA cm^{-2} led to significantly higher concentration of protein in the effluent solutions, which suggests that

some cells may be damaged even at relatively low voltages, causing intracellular protein leakage. As for the treatments at 5 and 10 mA cm^{-2}, the protein concentrations increased rapidly within the initial ten minutes, and then became stabilized. The increase in protein concentration was likely due to the increasing numbers of cell retained and subsequently inactivated on the membrane after being exposed to electric potential and ROS for a longer period of time. The similar pattern in hydraulic pressure change (**Figure S6**) predominately caused by bacterial mass accumulation on the membrane is an evidence of the increased cell retention at elevated current densities. Earlier studies indicated that longer exposure time to external electric field would cause more severe and lethal damages to the cells (Vecitis et al. 2011, Zeng et al. 2010).

Flow cytometry was employed in this study to assess the viability of cells during REM treatment in an effort to obtain a more comprehensive understanding of the different disinfection mechanisms. Flow cytometry measures the light scattering of a laser beam by stained cells, which is dependent on the viability of the cells (Nicoletti et al. 1991). When the measurement results of control samples prepared with live or dead cells were plotted according to their fluorescence signals, two regions (also called gates) are defined, which can serve as frame of references to differentiate the viable cells from inactivated ones. **Figure 5 s**hows the flow cytometry results of the effluent samples collected during different treatments, indicating the compositions of live and dead cells in each solution. Comparing to the live cell control, the percentage of dead cells increased dramatically at 1 mA cm^{-2} current density treatment, and it further increased when the current density raised to 5 mA cm^{-2}. This trend agreed well with the result from the plate count in that increasing the current density caused higher levels of damage and death to the cells.

However, it is important to note that, for both 1 and 5 mA cm^{-2} treatment, the percentage of "live" cells identified by flow cytometer was much higher than the results determined using the plate count method as shown in **Figure 2**. This difference may be caused by a fraction of cells that were detected as viable by flow cytometry as they still maintain the cell integrity, but have lost their ability to grow into a visible colony on agar plates due to serious injury. This fraction of cells can bring potential health risk once they recover with reproducibility or if their DNA remains intact. Therefore, it is critical to differentiate such cells from dead cells, while conducting disinfection study and evaluating disinfection efficiency. As implemented in this study, coupling flow cytometry and differential staining technique with direct microscopic enumeration can be an effective tool for such differentiation (Li et al. 2014).

The density of cells (represented by dots in **Figure 5**) was much lower in 10 mA cm^{-2} treatment than the other treatments, indicating that the treated effluent contained much less stainable cells. Bacterial cells became non-detectable to flow cytometry only when the cell membrane structure was completely altered or the whole cell broke into debris (Tung et al. 2007). Therefore, it is possible that the high current density might be vital to ensure complete destruction of bacteria cells and eliminate the possibility of pathogen recovery and disease spreading.

TEM was performed to investigate the *E. coli* cells in the effluents to provide information on cell morphology before and after REM treatments (**Figure 6**). For the zero-current control, the cells remained in their original rod shape with smooth membrane and intact cytoplasm (**Figure 6A**). Some changes in cell morphology occurred when voltage was added: for 1mA cm^{-2} treatment (**Figure 6B**), cell membrane became rougher; in 5 mA cm^{-2} sample (**Figure 6C**) some cells showed signs of cytoplasm leakage, although the cell membrane remained intact; when the

394 applied current density was increased to 10 mA cm^{-2} (**Figure 6D**), cell membrane started to
395 undergo dissociation and break into pieces. It was obvious that higher current density caused
396 more severe damages to the cells, leading to alteration of cell shape, leakage of cytoplasm, and,
397 more seriously, membrane disintegration. The mechanisms of cell inactivation by ROSs have
398 been described previously (Caselli et al. 1998, Cho et al. 2010, Nimse and Pal 2015). Generally,
399 ROSs will preferentially react with unsaturated membrane lipids and cause lipid peroxidation,
400 destructing membrane structure and cell integrity (Petersen 2017). Subsequently, ROSs can
401 diffuse through membrane and react with cytoplasmic proteins and unsaturated lipids. As a result,
402 affected cells may undergo lysis, and release cytoplasmic components into the surrounding
403 environment, causing elevated protein concentration in solution. Meanwhile, ROSs can infiltrate
404 through the membrane with altered permeability, and bond to the enzymes and DNA molecules
405 (Hunt and Mariñas 1999).

406 The results of SEM characterization of the treatment samples were highly consistent with
407 the observations made with the TEM images, showing cell shrinkage at moderate electrical
408 strength (1 and 5 mA cm^{-2}) (**Figure S8-B and S8-C**) while cells remaining intact at zero current
409 control (**Figure S8-A**). At 10 mA cm^{-2} treatment, cell membrane appeared to be rough with
410 visible damages on the surface (**Figure S8-D**). Although electroporation was considered another
411 effective mechanism in inactivating bacteria (Huo et al. 2016, Liu et al. 2013, Liu et al. 2014,
412 Wen et al. 2017), it unlikely played a significant role in the present study where low electric field
413 strengths (<10V) were applied. It is shown by SEM examination (**Figure S8**) that no pores were
414 evident on the cell membranes, suggesting the minimal effects of electroporation.

415 Large clusters of cell debris were found in the lower magnification SEM pictures of the
416 samples with 5 mA cm^{-2} and 10 mA cm^{-2} treatments (**Figure 6E and 6F**). This result again

417 suggested substantial leakage of intracellular material after electrolysis at high current densities,
418 and the leaked cellular components tend to aggregate into clusters of debris. Similar results were
419 reported by Bruguera-Casamada et al. (2016), who observed cell debris clusters in all the test
420 strains (*Escherichia coli*, *Pseudomonas aeruginosa*, *Bacillus atrophaeus*, *Staphylococcus aureus*,
421 and *Enterococcus hirae*) upon electrochemical disinfection treatment at a current density of 33.3
422 mA cm^{-2} in a batch reactor setup with BDD anode in 7 mM Na_2SO_4 solution.

423 4. Electrochemical inactivation of bacteriophage MS2

424 As shown in **Figure S9**, no lysis or plaques were observed in the plate inoculated with
425 effluent samples (10^{-6} dilution) of electrochemical filtration system at 10 mA cm^{-2} applied
426 current density; while with the same dilution rate, the suspension without treatment resulted in
427 scattered small plaques all over the plate. Based on the plate counting results of other plates with
428 lower dilution rates and countable number of plaques, the electrochemical removal of
429 bacteriophage MS2 was 6.74 log. Although the total inactivation rate is similar to bacteria study
430 (6.28 log), the inactivation of bacteriophage is considered more pronounced since the initial
431 concentration of bacteriophage (~10^{11}) is much higher than that of bacteria (~10^{6}). In general,
432 disinfection of pathogens at higher population is less effective due to the population-dependent
433 effect, which can be explained by the fact that a finite amount of oxidants would inactivate a
434 smaller portion of microorganisms at higher bacteria or phage population (Drees et al., 2003).
435 Besides inactivation by oxidizing agents generated during electrolysis, external electric field can
436 also inhibit the viability of bacteriophage. However, as non-enveloped virus, bacteriophage was
437 able to tolerate greater direct current magnitudes and longer time of exposure to direct current in
438 the electric field. Since ingesting even a single viral particle can potentially cause serious disease,

439 water disinfection/treatment system must be sufficiently effective to inactivate pathogenic
440 viruses to none-health threatening level.

441 **Conclusions**

442 An electrochemical dead-end filtration system consisting of two highly conductive, stable,
443 and porous titanium sub-oxide electrodes were demonstrated in this study to effectively
444 inactivate *E. coli* and bacteriophage MS2 in water. The highest inactivation rates were 6.28 log
445 for bacteria and 6.74 log for bacteriophage at the current density of 10 mA cm^{-2}. Under the same
446 electrochemical conditions, the inactivation study was also conducted in a batch reactor, and the
447 results revealed that effective inactivation of cells happened only when the anodic potential was
448 higher than the oxygen evolution potential. This suggested the dominant role of oxidizing species,
449 especially hydroxyl radicals, which were generated in great amount during oxygen evolution, in
450 the REM treatment system.

451 Detailed investigation was performed to elucidate the bacteria inactivation mechanism
452 using multi-tool approach including membrane pressure monitoring, plate cell counting, protein
453 leakage quantification, and SEM and TEM scanning. In general, higher current density led to
454 greater reduction of bacteria concentration and more severe damage to the cells, causing
455 significant protein leakage and altered cell membrane structure or even cell disintegration as the
456 treatment intensity increased. An array of mechanisms works synergistically to disinfect *E. Coli*
457 in this electrochemical treatment system, namely physical separation and entrapment, external
458 electrical field disturbance, and predominately, injuries caused by oxidants produced on the
459 anode. The impact of electroporation is considered minimum with the absence of holes on cell
460 membrane shown in the SEM and TEM images. Flow cytometry analysis revealed that viable but
461 non-culturable cells are present in the samples treated at low current densities, and they can be

462 effectively controlled at high current density (i.e. 10 mA cm^{-2}). Although lacking reproducibility,
463 pathogenic bacteria with integrated cell structure still carry health risk to water consumers under
464 exposure and thus must be eliminated in disinfection system. The results of this study indicate
465 that the novel porous titanium suboxide electrode with high flux rate and extraordinary
466 electrochemical performance makes REM a promising option to meet decentralized water
467 disinfection demands.

468 **Acknowledgements:**

469 The research is supported in part by U.S. Department of Defense SERDP ER2717 (W912HQ-17-
470 C-0010). Mr. Xi Chen and Mr. George Kwabena Afari are acknowledged for assistance with
471 flow cytometry.

References

Belháčová, L., Krýsa, J., Geryk, J. and Jirkovský, J., 1999. Inactivation of microorganisms in a flow-through photoreactor with an immobilized TiO_2 layer. Journal of Chemical Technology and Biotechnology 74(2), 149-154.

Boudreau, B. P., 1996. The diffusive tortuosity of fine-grained unlithified sediments. Geochimica et Cosmochimica Acta 60(16), 3139-3142.

Brady-Estévez, A.S., Schnoor, M.H., Vecitis, C.D., Saleh, N.B. and Elimelech, M., 2010. Multiwalled carbon nanotube filter: improving viral removal at low pressure. Langmuir 26(18), 14975-14982.

Bruguera-Casamada, C., Sirés, I., Prieto, M.J., Brillas, E. and Araujo, R.M., 2016. The ability of electrochemical oxidation with a BDD anode to inactivate Gram-negative and Gram-positive bacteria in low conductivity sulfate medium. Chemosphere 163, 516-524.

Caselli, A., Marzocchini, R., Camici, G., Manao, G., Moneti, G., Pieraccini, G. and Ramponi, G. (1998) The inactivation mechanism of low molecular weight phosphotyrosine-protein phosphatase by H_2O_2. Journal of Biological Chemistry 273(49), 32554-32560.

Cho, M., Kim, J., Kim, J.Y., Yoon, J. and Kim, J.-H., 2010. Mechanisms of *Escherichia coli* inactivation by several disinfectants. Water Research 44(11), 3410-3418.

Cui, X., Quicksall, A.N., Blake, A.B. and Talley, J.W., 2013. Electrochemical disinfection of *Escherichia coli* in the presence and absence of primary sludge particulates. Water Research 47(13), 4383-4390.

de Lannoy, C.-F.o., Jassby, D., Gloe, K., Gordon, A.D. and Wiesner, M.R., 2013. Aquatic biofouling prevention by electrically charged nanocomposite polymer thin film membranes. Environmental Science and Technology 47(6), 2760-2768.

Ding, T., Suo, Y., Xiang, Q., Zhao, X., Chen, S., Ye, X. and Liu, D., 2017. Significance of viable but nonculturable *Escherichia coli*: induction, detection, and control. Journal of Microbiology and Biotechnology 27(3), 417-428.

Drees, K.P., Abbaszadegan, M. and Maier, R.M., 2003. Comparative electrochemical inactivation of bacteria and bacteriophage. Water Research 37(10), 2291-2300.

Elangovan, M., and Dharmalingam, S., 2017. Anti-biofouling anion exchange membrane using surface modified quaternized poly (ether imide) for microbial fuel cells. Journal of Applied Polymer Science 134(5).

Enache, T.A., Chiorcea-Paquim, A.-M., Fatibello-Filho, O. and Oliveira-Brett, A.M., 2009. Hydroxyl radicals electrochemically generated in situ on a boron-doped diamond electrode. Electrochemistry Communications 11(7), 1342-1345.

Fakruddin, M., Mannan, K.S.B. and Andrews, S., 2013. Viable but nonculturable bacteria: food safety and public health perspective. ISRN Microbiology 2013.

Fernández-Ibáñez, P., Blanco, J., Malato, S. and De Las Nieves, F., 2003. Application of the colloidal stability of TiO_2 particles for recovery and reuse in solar photocatalysis. Water Research 37(13), 3180-3188.

Ficek, M., Sobaszek, M., Gnyba, M., Ryl, J., Smietana, M., Jasiński, J., and Bogdanowicz, R., 2016. Optical and electrical properties of boron doped diamond thin conductive films deposited on fused silica glass substrates. Applied Surface Science 387, 846-856.

Garcia, P.A., Ge, Z., Moran, J.L. and Buie, C.R., 2016. Microfluidic screening of electric fields for electroporation. Scientific Reports 6, 21238.

Geveke, D. and Kozempel, M., 2003. Pulsed electric field effects on bacteria and yeast cells. Journal of Food Processing and Preservation 27(1), 65-72.

Gkotsis, P.K., Banti, D.C., Peleka, E.N., Zouboulis, A.I. and Samaras, P.E., 2014. Fouling issues in membrane bioreactors (MBRs) for wastewater treatment: major mechanisms, prevention and control strategies. Processes 2(4), 795-866.

Guo, L., Ding, K., Rockne, K., Duran, M. and Chaplin, B.P., 2016. Bacteria inactivation at a sub-stoichiometric titanium dioxide reactive electrochemical membrane. Journal of Hazardous Materials 319, 137-146.

Huang, X., Qu, Y., Cid, C.A., Finke, C., Hoffmann, M.R., Lim, K. and Jiang, S.C., 2016. Electrochemical disinfection of toilet wastewater using wastewater electrolysis cell. Water Research 92, 164-172.

Hunt, N.K. and Mariñas, B.J., 1999. Inactivation of *Escherichia coli* with ozone: chemical and inactivation kinetics. Water Research 33(11), 2633-2641.

Huo, Z.-Y., Xie, X., Yu, T., Lu, Y., Feng, C. and Hu, H.-Y., 2016. Nanowire-Modified Three-Dimensional Electrode Enabling Low-Voltage Electroporation for Water Disinfection. Environmental Science and Technology 50(14), 7641-7649.

Jeong, J., Kim, C. and Yoon, J., 2009. The effect of electrode material on the generation of oxidants and microbial inactivation in the electrochemical disinfection processes. Water Research 43(4), 895-901.

Kikuchi, Y., Sunada, K., Iyoda, T., Hashimoto, K. and Fujishima, A., 1997. Photocatalytic bactericidal effect of TiO_2 thin films: dynamic view of the active oxygen species responsible for the effect. Journal of Photochemistry and Photobiology A: Chemistry 106(1), 51-56.

Kong, C.S., Kim, D.-Y., Lee, H.-K., Shul, Y.-G. and Lee, T.-H., 2002. Influence of pore-size distribution of diffusion layer on mass-transport problems of proton exchange membrane fuel cells. Journal of Power Sources 108(1), 185-191.

Leiknes, T., Ødegaard, H. and Myklebust, H., 2004. Removal of natural organic matter (NOM) in drinking water treatment by coagulation–microfiltration using metal membranes. Journal of Membrane Science 242(1), 47-55.

Li, L., Mendis, N., Trigui, H., Oliver, J.D. and Faucher, S.P., 2014. The importance of the viable but non-culturable state in human bacterial pathogens. Frontiers in Microbiology 5.

Li, Y., Kemper, J.M., Datuin, G., Akey, A., Mitch, W.A. and Luthy, R.G., 2016. Reductive dehalogenation of disinfection byproducts by an activated carbon-based electrode system. Water Research 98, 354-362.

Liang, S., Lin, H., Yan, X., and Huang, Q., 2018. Electro-oxidation of tetracycline by a Magnéli phase Ti_4O_7 porous anode: Kinetics, products, and toxicity. Chemical Engineering Journal 332, 628-636.

Liu, C., Xie, X., Zhao, W., Liu, N., Maraccini, P.A., Sassoubre, L.M., Boehm, A.B. and Cui, Y., 2013. Conducting nanosponge electroporation for affordable and high-efficiency disinfection of bacteria and viruses in water. Nano Letters 13(9), 4288-4293.

Liu, C., Xie, X., Zhao, W., Yao, J., Kong, D., Boehm, A.B. and Cui, Y., 2014. Static electricity powered copper oxide nanowire microbicidal electroporation for water disinfection. Nano Letters 14(10), 5603-5608.

Long, Y., Ni, J. and Wang, Z., 2015. Subcellular mechanism of *Escherichia coli* inactivation during electrochemical disinfection with boron-doped diamond anode: A comparative study of three electrolytes. Water Research 84, 198-206.

562 Machado, L.F., Pereira, R.N., Martins, R.C., Teixeira, J.A. and Vicente, A.A., 2010. Moderate
563 electric fields can inactivate *Escherichia coli* at room temperature. Journal of Food
564 Engineering 96(4), 520-527.
565 Maness, P.-C., Smolinski, S., Blake, D.M., Huang, Z., Wolfrum, E.J. and Jacoby, W.A., 1999
566 Bactericidal activity of photocatalytic TiO_2 reaction: toward an understanding of its
567 killing mechanism. Applied and Environmental Microbiology 65(9), 4094-4098.
568 Marselli, B., Garcia-Gomez, J., Michaud, P.-A., Rodrigo, M. and Comninellis, C., 2003.
569 Electrogeneration of hydroxyl radicals on boron-doped diamond electrodes. Journal of
570 the Electrochemical Society 150(3), D79-D83.
571 Marty, A., Causserand, C., Roques, C., and Bacchin, P., 2014. Impact of tortuous flow on
572 bacteria streamer development in microfluidic system during filtration. Biomicrofluidics
573 8(1), 014105.
574 McCleskey, R.B., Nordstrom, D.K. and Ryan, J.N., 2011. Electrical conductivity method for
575 natural waters. Applied Geochemistry 26, S227-S229.
576 Nicoletti, I., Migliorati, G., Pagliacci, M., Grignani, F. and Riccardi, C., 1991. A rapid and
577 simple method for measuring thymocyte apoptosis by propidium iodide staining and flow
578 cytometry. Journal of Immunological Methods 139(2), 271-279.
579 Nimse, S.B. and Pal, D., 2015. Free radicals, natural antioxidants, and their reaction mechanisms.
580 Rsc Advances 5(35), 27986-28006.
581 Olson, M. S., Ford, R. M., Smith, J. A., and Fernandez, E. J., 2005. Analysis of column
582 tortuosity for $MnCl_2$ and bacterial diffusion using magnetic resonance imaging.
583 Environmental Science and Technology, 39(1), 149-154.
584 Organization, W.H., 2015. Progress on sanitation and drinking water: 2015 update and MDG
585 assessment, World Health Organization.
586 Petersen, R. C., 2017. Free-radicals and advanced chemistries involved in cell membrane
587 organization influence oxygen diffusion and pathology treatment. AIMS Biophysics 4(2),
588 240.
589 Pillet, F., Formosa-Dague, C., Baaziz, H., Dague, E. and Rols, M.-P., 2016. Cell wall as a target
590 for bacteria inactivation by pulsed electric fields. Scientific Reports 6, 19778.
591 Presser, K., Ratkowsky, D. and Ross, T., 1997. Modelling the growth rate of *Escherichia coli* as
592 a function of pH and lactic acid concentration. Applied and Environmental Microbiology
593 63(6), 2355-2360.
594 Rahaman, M.S., Vecitis, C.D. and Elimelech, M., 2012 Electrochemical carbon-nanotube filter
595 performance toward virus removal and inactivation in the presence of natural organic
596 matter. Environmental Science and Technology 46(3), 1556-1564.
597 Rajab, M., Heim, C., Letzel, T., Drewes, J.E. and Helmreich, B., 2015. Electrochemical
598 disinfection using boron-doped diamond electrode–The synergetic effects of in situ ozone
599 and free chlorine generation. Chemosphere 121, 47-53.
600 Rajeshwar, K., Ibanez, J. and Swain, G., 1994. Electrochemistry and the environment. Journal of
601 Applied Electrochemistry 24(11), 1077-1091.
602 Raut, A.S., Cunningham, G.B., Parker, C.B., Klem, E.J., Stoner, B.R., Deshusses, M.A. and
603 Glass, J.T., 2014. Disinfection of *E. coli* contaminated urine using boron-doped diamond
604 electrodes. Journal of the Electrochemical Society 161(12), G81-G85.
605 Reed, R.H., 2004. The inactivation of microbes by sunlight: solar disinfection as a water
606 treatment process. Advances in Applied Microbiology 54, 333-365.

Särkkä, H., Vepsäläinen, M., Pulliainen, M. and Sillanpää, M., 2008. Electrochemical inactivation of paper mill bacteria with mixed metal oxide electrode. Journal of Hazardous Materials 156(1), 208-213.

Schaefer, C.E., Andaya, C. and Urtiaga, A., 2015. Assessment of disinfection and by-product formation during electrochemical treatment of surface water using a Ti/IrO_2 anode. Chemical Engineering Journal (Lausanne) 264, 411-416.

Schmalz, V., Dittmar, T., Haaken, D. and Worch, E., 2009. Electrochemical disinfection of biologically treated wastewater from small treatment systems by using boron-doped diamond (BDD) electrodes–Contribution for direct reuse of domestic wastewater. Water Research 43(20), 5260-5266.

Smith, A.R., Ellison, A.L., Robinson, A.L., Drake, M., McDOWELL, S.A., Mitchell, J.K., Gerard, P.D., Heckler, R.A. and McKILLIP, J.L., 2013. Enumeration of sublethally injured Escherichia coli O157: H7 ATCC 43895 and Escherichia coli strain B-41560 using selective agar overlays versus commercial methods. Journal of Food Protection 76(4), 674-679.

Smith, J., Walsh, F. and Clarke, R., 1998. Electrodes based on Magnéli phase titanium oxides: the properties and applications of Ebonex® materials. Journal of Applied Electrochemistry 28(10), 1021-1033.

Sultana, S.T., Babauta, J.T. and Beyenal, H., 2015. Electrochemical biofilm control: a review. Biofouling 31(9-10), 745-758.

Tung, J.W., Heydari, K., Tirouvanziam, R., Sahaf, B., Parks, D.R., Herzenberg, L.A. and Herzenberg, L.A., 2007. Modern flow cytometry: a practical approach. Clinics in Laboratory Medicine 27(3), 453-468.

Vecitis, C.D., Schnoor, M.H., Rahaman, M.S., Schiffman, J.D. and Elimelech, M., 2011. Electrochemical multiwalled carbon nanotube filter for viral and bacterial removal and inactivation. Environmental Science and Technology 45(8), 3672-3679.

Wen, J., Tan, X., Hu, Y., Guo, Q. and Hong, X., 2017. Filtration and electrochemical disinfection performance of PAN/PANI/AgNWs-CC composite nanofiber membrane. Environmental Science and Technology.

Zaky, A.M. and Chaplin, B.P., 2014. Mechanism of p-substituted phenol oxidation at a Ti_4O_7 reactive electrochemical membrane. Environmental Science and Technology 48(10), 5857-5867.

Zeng, X., Tang, W., Ye, G., Ouyang, T., Tian, L., Ni, Y. and Li, P., 2010. Studies on disinfection mechanism of electrolyzed oxidizing water on *E. coli* and Staphylococcus aureus. Journal of Food Science 75(5).

Table 1. Summary of current density, applied voltage, live cells in effluent, live cells retained on membrane, and total inactivation rate of *E. coli* by REM system.

Current density (mA cm^{-2})	Applied voltage (V)	Log reduction	Live cells in effluent (%)	Live cells on membrane (%)	Total removal (%)	Energy consumption (kWh/m^3)
0	0.0	2.52	0.303	0.057	99.640 ± 0.042	0.00
1	6.4	3.01	0.096	0.010	99.895 ± 0.046	0.21
5	7.6	4.88	0.001	0.018	99.981 ± 0.100	1.26
10	9.5	6.28	0.000	0.000	99.998 ± 0.012	3.18

Note: All percentage values were compared to the number of cells pumped into filtration system from feed tank during 30 minutes' treatment.

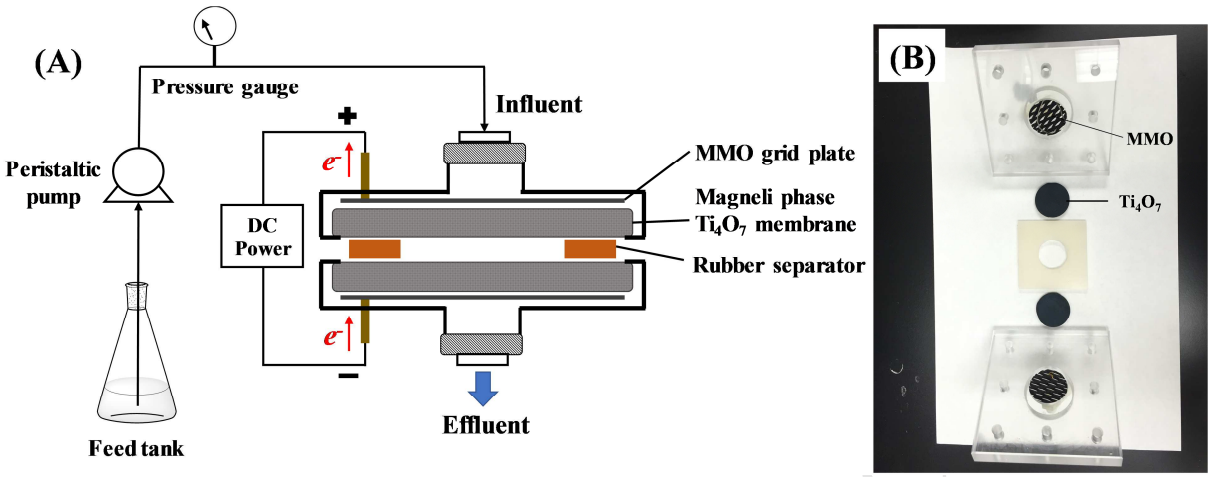

Figure 1. (A) Electrochemical Magnéli phase Ti_4O_7 ceramic membrane filtration system design and setup; (B) Picture of the real filtration device. The diameter of Magnéli phase Ti_4O_7 ceramic membrane disk electrodes is 3 cm.

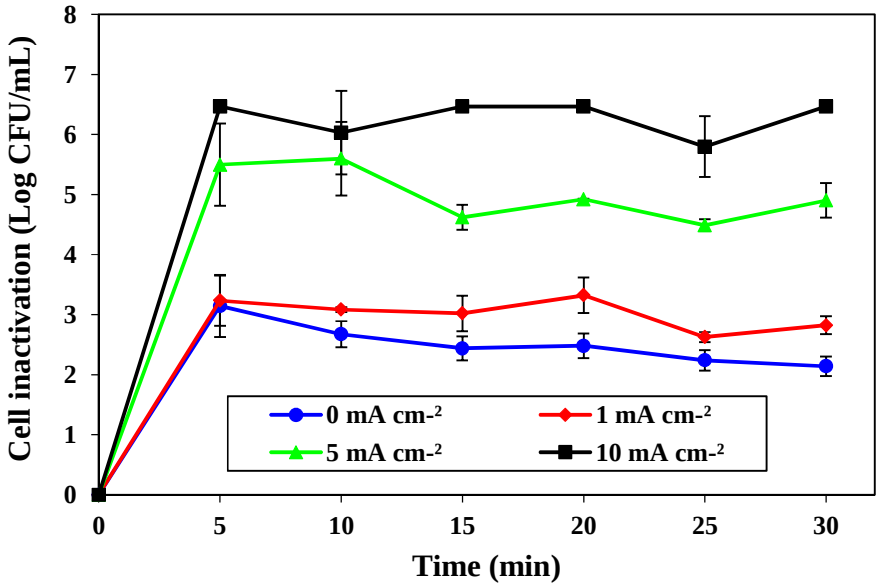

Figure 2. Removal of *E. coli* by Magnéli phase Ti_4O_7 membrane filtration system at different current densities.

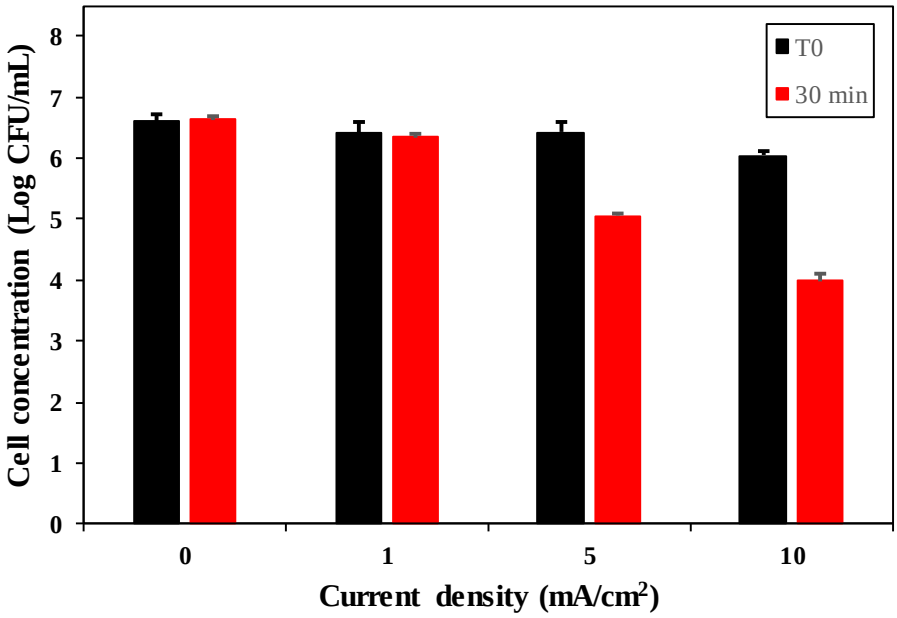

Figure 3. Removal of *E. coli* using Magnéli phase Ti_4O_7 membrane in batch reactor at different current density after 30 mins.

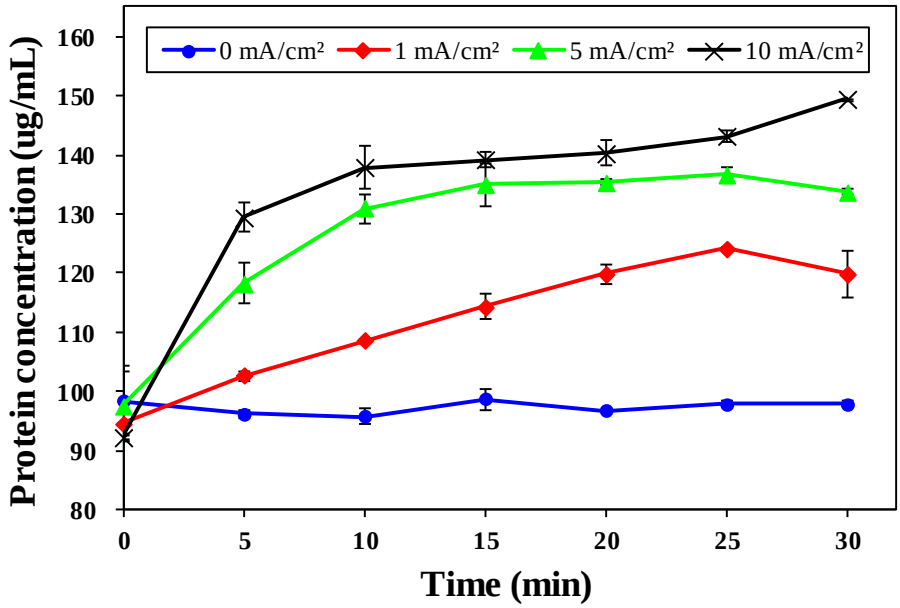

Figure 4. Leakage of proteins from *E. coli* cells after electrochemical disinfection treatments by REM at different current densities.

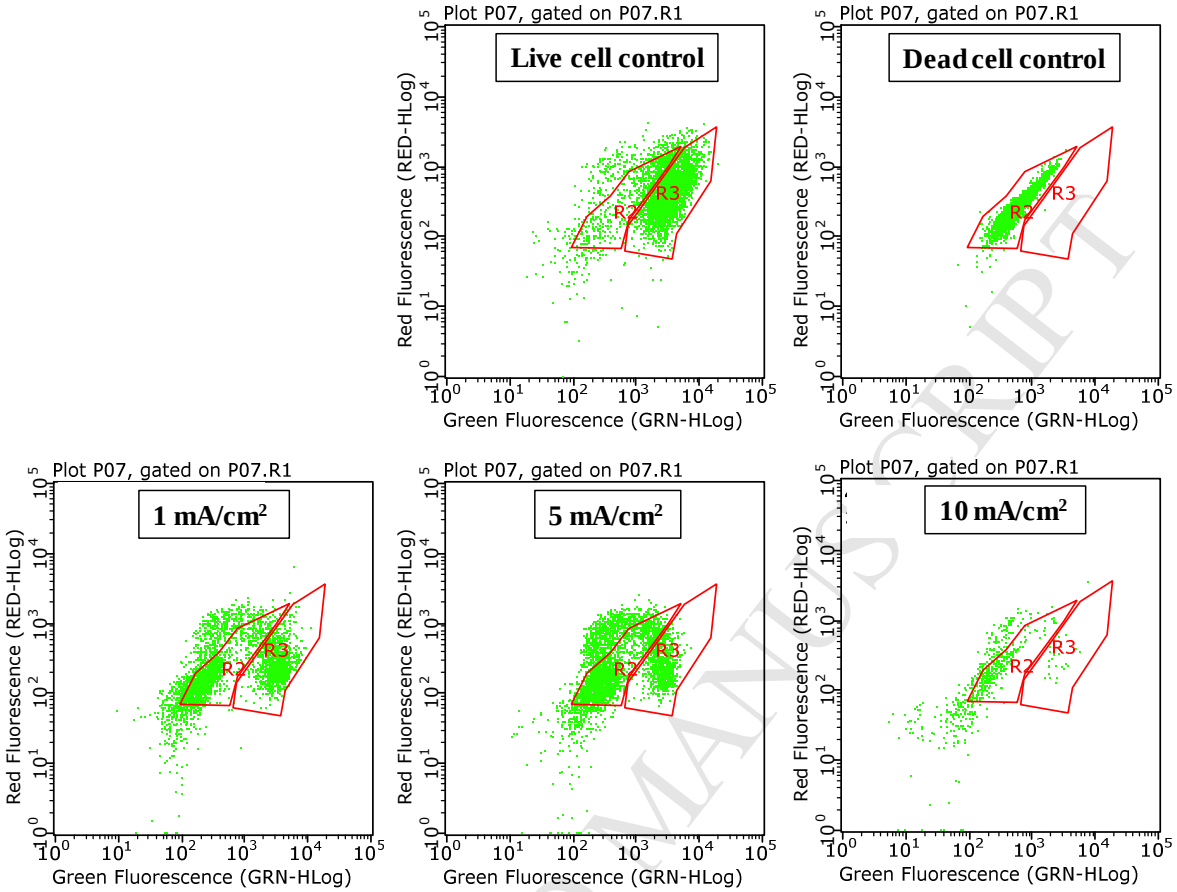

Figure 5. Flow cytometry analysis of effluent samples collected during electrochemical disinfection process for treating *E. coli* at different current density. Every cell that passes flow cytometer and is detected will be presented as single green dot on a scatter plot. Green dots within gate R2 represent the subpopulation of dead cells. Green dots within gate R3 represent the subpopulation of live cells.

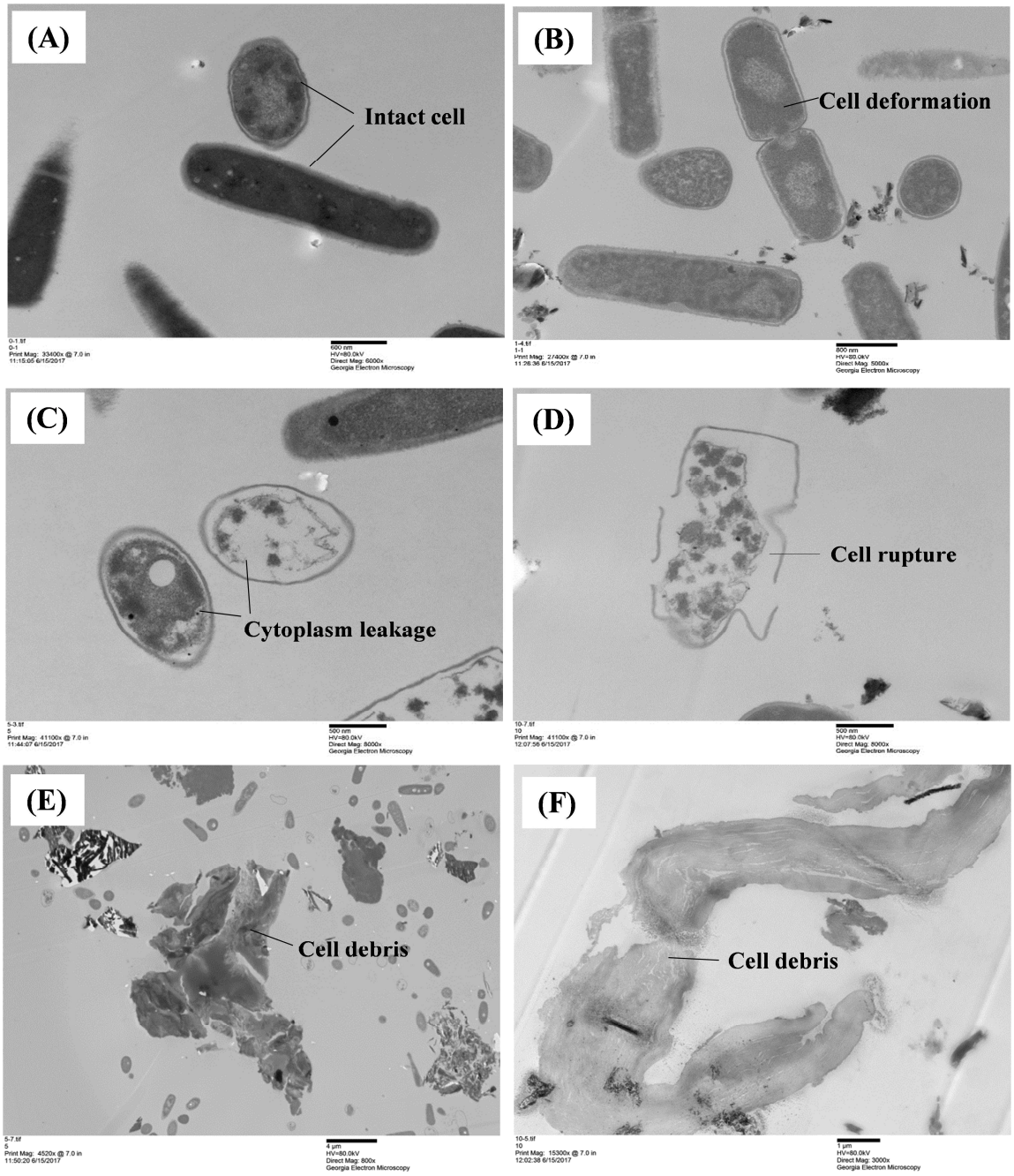

Figure 6. TEM images of effluent samples collected during electrochemical disinfection process. (A) No current control; (B) 1 mA cm^{-2} applied current density; (C) 5 mA cm^{-2}applied current density; (D) 10 mA cm^{-2} applied current density; (E) Cell debris observed in 5 mA cm^{-2} treatment sample; (F) Cell debris observed at 10 mA cm^{-2} treatment sample.

Highlights

- A novel electrochemical filtration system with titanium suboxide membrane was developed.
- Effective disinfection of E. coli and bacteriophage MS2 in water was achieved.
- The disinfection mechanism on titanium suboxide anode was elucidated.
- The system is potentially promising for decentralized water disinfection applications.